

Action Mechanism of Molecular Iodine Complex with Bioorganic Ligands, Magnesium and Lithium Halogenides on Human Tuberculosis Strain With Multiple Drug Resistance

Ilin A, Kerimzhanova B and Yuldasheva G*

The Scientific Center for Anti-infectious Drugs, Republic of Kazakhstan

Abstract

Findings of a research on antibacterial effects of a newly synthesized iodine-containing drug (FS-1) against both the drug susceptible strain *Mycobacterium tuberculosis* H₃₇Rv and an isolate of *M. tuberculosis* MS-115 with a multiple drug resistance phenotype, were discussed. The obtained results of the microbiological studies confirmed a bactericidal activity of FS-1 against sensitive and multi-drug resistant strains of *M. tuberculosis* at the concentrations from 8.2 µg/mL to 2.7 µg/mL during the entire investigation period (42 h).

Spectrophotometry has shown that FS-1 causes changes in the permeability of the cell membrane of mycobacteria. Also it penetrates through the cytoplasmic membrane and causes the lysis of the cells (spheroplasts) partially devoid of the cell wall.

Antibacterial action mechanism was studied by using the technique of the molecular modeling. Particularly, the DFT/CAM-B3LYP density potential approach has shown that the active center of FS-1, which contains magnesium ion, destroys the active catalytic complex of the DNA-dependent RNA polymerase (RNAP) and can disrupt in this way the transcription of bacterial RNA. Active center of FS-1 becomes a center of new nucleoprotein complex, which binds both the bacterial DNA and the ion Mg²⁺(COO)⁻³ within the catalytic RNAP complex. The conditions responsible for vital processes in the bacterial cell are violated. As a result, a cell lysis is observed.

Keywords: *Mycobacterium tuberculosis*; Bacterial RNA; Microbiological studies

Introduction

Infectious diseases at the beginning of the XXI century pose the most challenging problem and inflict significant damage to mankind. Tuberculosis is one of the most extensive contagious diseases in all the countries across the world. The spread of *Mycobacterium tuberculosis* (MT) strains with multiple drug resistance (MDR) is a hazard requiring the highest priority. The formation of germicidal drug resistance among infectious agents leads to the reduction or total loss of the therapeutic efficiency, and, thus, raises the problem of search for new pharmaceutical drugs. Development of new drug-producing techniques these days stands as the crucial and topical problem.

Use of iodine-containing drugs against infectious agents represents one of the options to overcome the given problem. Iodine is characterized by a high bioactivity and exerts wide antimicrobial spectrum with no recorder evidences of resistance development to iodine in bacteria and viruses. The new anti-infectious drug (FS-1) containing molecular iodine has been recently created [1].

This article provides the results on *in vitro* studies on the impact of FS-1 on tuberculosis agents including a MDR strain compared to the reference strain that is susceptible to anti-mycobacterial drugs.

FS-1 is an aqueous solution of a polymer complex, which contains molecular iodine as well as potassium lithium, magnesium halogenides, polypeptides and α -dextrin. Using the methods of molecular modeling based on the results of UV and IR-spectroscopy, we suggested the structure of three active centers of FS-1, located within α -dextrin helix and forming complexes with α -dextrin helix: molecular iodine complex with lithium halogenides and polypeptides (LiCl(I)₂polypeptdex), lithium halogenide (LiCl(I)) and triiodide (I₃⁻) [2].

The magnesium ions, which are components of FS-1, can also

penetrate the α -dextrin helix and form complex with triiodide and LiCl(I)₂polypeptdex. Content of magnesium ions in FS-1 is significantly less than that of LiCl and I₂. For this reason, the three active complexes given above and the Mg²⁺I₃LiCl(I)₂polypeptdex complexes can be found in α -dextrin helix. In this article, we study the structure of the fourth active center of FS-1 and its impact on the antibacterial effect of FS-1.

Understanding of the mechanisms of suppression of drug resistant *M. tuberculosis* growth will stimulate discovery of a new drug.

In this article we have shown that Mg²⁺I₃LiCl(I)₂polypeptdex complex inhibits the active center of DNA-dependent RNA-polymerase of *M. tuberculosis*. FS-1 destroys the active catalytic center of DNA-dependent RNA-polymerase (RNAP) and then acts as the center of a new nucleoprotein complex that binds both bacterial DNA and ion (Mg(COO)₃) component from the active catalytic center.

Materials and Methods

The study includes the reference strain of human tuberculosis agent, *M. tuberculosis* H37Rv, which is susceptible to antituberculous drugs and a multi-drug resistant clinical isolate M-115. These strains were

*Corresponding author: Yuldasheva G, The Scientific Center for Anti-infectious Drugs, Republic of Kazakhstan, Tel: 77272665229; E mail: yuldasheva57@rambler.ru

Received November 14, 2017; Accepted December 05, 2017; Published December 12, 2017

Citation: Ilin A, Kerimzhanova B, Yuldasheva G (2017) Action Mechanism of Molecular Iodine Complex with Bioorganic Ligands, Magnesium and Lithium Halogenides on Human Tuberculosis Strain With Multiple Drug Resistance. J Microb Biochem Technol 9:293-300. doi: [10.4172/1948-5948.1000381](https://doi.org/10.4172/1948-5948.1000381)

Copyright: © 2017 Ilin A, et al. This is an open-access article distributed under the terms of the Creative Commons Attribution License, which permits unrestricted use, distribution, and reproduction in any medium, provided the original author and source are credited.

received from the collection of Central tuberculosis scientific research institute of the Russian academy of medical sciences.

Cultivation of the strains of mycobacteria in the presence of FS-1 on a computer controlled system

Bactec MGIT 960: Determination of the anti-tuberculous activity was performed using the computer-based system Bactec MGIT 960. Antibacterial action of the drug was studied pursuant to the dynamics of culture growth placed in enriched liquid medium Middlebrook 7H9 under experimental concentrations of FS-1 of 8,2, 4,1, 2,7, 2,1, 1,6 µg/ml. The strain growth in the medium without drug served was used as the negative control and the growth on the medium supplemented with 0.1 µg/ml isoniazid was the positive control.

Growth detection was observed via computer-aided system of the culture growth recording MGIT 960. Mycobacterium growth detection was performed hly using Epicenter (Becton Dickinson) software. The dynamics of mycobacterium cellular fission was recorded in fluorescent relative units. Bacterial growth was controlled also by a visual inspection of positive test tubes (medium transparence, the presence of stippling and culture cloud on the bottom of test tube), smear microscopy, Ziehl-Neelsen staining and DNA-identification (PCR per IS6110). Mathematical treatment of findings and graphic representation of numeric test data was performed using standard statistical package Microsoft Office Excel.

The permeability of the membrane of mycobacterial cells under the impact of FS-1

Permeability testing of intact cells was implemented according to the technique based on the spectrophotometric measurement of the release of low-molecular compounds from bacterial cells [3]. Collection strain *M. smegmatis* ATCC 607 received from the American Type Culture Collection (ATCC) was used as a model microorganism. Cultivation of tested microbial strains was performed in liquid nutrient medium. Collection of the bacterial growth was carried out at the beginning of the stationary growth phase by centrifugation. Bacterial suspension was prepared in the physiological solution with the neutral pH (pH=7.0) and controlled by the turbidity standard (number of microbial bodies in suspension (NMB)) equal to 1.5×10^8 NMB/ml. The following FS-1 concentrations were used in the work: 100, 64, 32, 16, 8, 4 and 2 µg/mL.

The suspension of *M. smegmatis* served as a positive control processed with the standard buffer solution (Perm Buffer), which invariably increases membrane permeability. No FS-1 was added in the negative control. There were also remaining "Probe" represented by the tested FS-1 concentrations on normal saline solutions, which were automatically and instrumentally deducted as a background noise. For the negative control, a pure normal saline solution was used as a blank and buffer solution of Perm Buffer served for the positive control. The release of low-molecular compounds was detected via measurement of changes in the optical density of supernatant using plan-table photometer Multiscan ascent and Smart Spec Plus spectrophotometer, at the wavelength of 260-280 nm. The obtained experimental results were expressed in a percentage of the ratio to the negative control accounted for 100%.

Membranolytic activity of the drug FS-1 on spheroplasts of *M. smegmatis*.

Determination of the FS-1 membranolytic activity was implemented on *M. smegmatis* ATCC 607 spheroplasts [3]. Spheroplasts were obtained by the treatment of bacterial cells by lysozyme. 100% spheroplast formation was controlled with the use of smear microscopy based on phase-contrast method.

The following concentrations of FS-1 were used in this experiment: 100, 64, 32, 16, 8, 4 and 2 µg/mL. Suspension of spheroplast unexposed to FS-1 served as a negative control.

The measurement of optical density of spheroplasts was implemented on Lambda 35 (Perkin Elmer, USA) spectrophotometer at the wavelength of 540 nm during 30 min at 5 min interval.

Electronmicroscopy

Electron microscopy of cells of *M. tuberculosis* treated by the drug FS-1 was performed on the JEM-1011 transmission microscope (Japan). In this experiment the *M. tuberculosis* strain 320 with drug resistance to rifampicin, isoniazid, streptomycin, ethambutol and pyrazinamide was used [4].

Bacterial culture mass from Lowenstein-Jensen medium exposed to FS-1 drug at a dilution of 1:50 was fixed by 2.5% glutaric dialdehyde in 0.1 M in phosphate buffer with pH 7.2 during 2 h. Then the samples were washed out for 2 times in the same buffer and were placed for 3 hs in 1% osmium tetroxide solution (O_8O_4). Later on these specimens were washed out for 3 times in 50% ethanol (until solution becomes transparent). The samples were left overnight at 4°C in 2% uranyl acetate solution in 70% ethanol. Subsequent experiments were performed in rising ethanol concentrations: In 80%- 2 times for 30 min; in 96%- once for 1 h; in absolute alcohol (100%) for 1 h. Then they were dehydrated in absolute (abs.) acetone for 2 times during 30 min. Slice on formvar films were examined under transmission microscope with the accelerating voltage of 80 kV after being contrasted by uranyl acetate with Reynolds's reagent.

Molecular modeling

Structures modeling the mechanism of antibacterial action of FS-1 are calculated using the DFT/CAM-B3LYP approach [4]. Calculations were carried out using the GAUSSIAN 09 [5].

Results

Cultivation of the strains of Mycobacteria in the presence of PS-1 on the computer based system

Bactec MGIT 960: Table 1 shows the results of the antibacterial action of FS-1 during the growth of *M. tuberculosis* H₃₇Rv, *M. tuberculosis* MS-115 mycobacterium culture growth in Middlebrook 7H10 enriched liquid medium for 42 days.

The study of the FS-1 anti-bacterial activity by cultivation of the strains in the Bactec MGIT 960 computer-aided system demonstrated that FS-1 exerts a strong activity against *M. tuberculosis* the collection

Stain	Concentration FS-1, µg/mL					Isoniazid 0.1 µg/mL	NC
	8.2	4.1	2.7	2.1	1.6		
<i>M. tuberculosis</i> H ₃₇ Rv	-	-	-	+	+	-	+
<i>M. tuberculosis</i> MS-115	-	-	-	+	+	+	+

«NC» -negative control, «+» bacterial cell growth, «-» bacterial cell growth absent

Table 1: Antituberculous activity of FS-1.

strain H₃₇Rv in concentration from 8.2 to 2.7 µg/mL. At these concentrations throughout the entire study period the FS-1 drug showed an equally strong germicidal activity against the MDR strain *M. tuberculosis* MS-115. The latter strain was resistant to rifampicin, isoniazid, streptomycin, ethambutol and pyrazinamide. In the given experiment, growth of the strain *M. tuberculosis* MS-115 was observed in the positive control reference medium containing isoniazid starting from the 6th day of cultivation.

The permeability of the membrane of mycobacterial cells under the impact of FS-1.

It is known that iodine can disrupt structures of bacterial transmembrane proteins and enzymes if they are not protected by cell membranes [6,7]. Oxidation of the transmembrane proteins by iodine leads to a structural degeneration followed by loss of their functionality. Moreover, oxidation of membranous phospholipids by iodine results in an increased mobility of polar -N⁺-(CH₃)₃ groups and increased C-C coupling rotations, which, in turn, leads to an acceleration of the lateral molecular diffusion through the membrane [8].

Several authors also suggested that the lipid oxidation might result in a reduction of the strength of lipid-protein interactions that would facilitate a lipid membrane release and, thus, can lead to bacterial cell lysis [9,10].

According to the literature data, bacterial cell releases in situ various genetic elements (transposons, transposable genetic elements, RNA) and adenosine triphosphate (ATP), adenosine diphosphate (ADP) and adenosine monophosphate (AMP) within its environment and the molecular mass of these elements does not exceed 900 Da [11]. These compounds are strongly lipophilic, which means that they are highly soluble in lipids and, thus, may facilitate permeability of the lipid bilayer of cell membranes [12]. Because of the naturally multifold or tenfold higher intracellular osmotic pressure in bacterial cells, the increased bacterial membrane permeability causes an increased release of the lipophilic low-molecular compounds from the cells. Thus, observation of an increased release of these compounds from cells in an experiment can indicate an increased permeability of cytoplasmic membranes.

In that context we studied the impact of FS-1 on the bacterial cell structures in the experiment on *M. smegmatis*. Data on the cell membrane permeability after the exposure to various FS-1 drug concentrations obtained by a spectrophotometric detection of the release of low-molecular compound from bacterial cell are given in Figure 1.

The study of the drug impact on intact cells has demonstrated that all the tested concentration of FS-1 ranging from 8 µg/mL to 100 µg/mL increased the release of low-molecular compounds into the culture liquid. Hence, the drug exposure at the concentration of 10 µg/mL increased the release of the low-weight molecular compounds by 159.3% and at the concentration of 64 µg/mL the increase was 143.2%; whereas the concentrations of 32 µg/mL and 16 µg/mL increased the release by 72.3% and 23.7%, respectively. The drug impact at the concentration of 8 µg/mL increased the release by 21.3%.

These findings are indicative of the fact that FS-1 substantially increases permeability of the cell membrane.

Membranolytic activity of the drug FS-1 on spheroplasts *M. smegmatis*

Cytoplasmic membrane is located under cell wall in bacterial cells. One of the main functions of the cytoplasmic membrane consists in

allowing many bacterial cell processes including the cell breathing and division. For this reason, the next stage of the study was comprised of an investigation of the FS-1 drug membranolytic activity on spheroplasts, i.e., on cells partially lacking the cell walls.

A suspension of spheroplasts of the *M. smegmatis* culture was prepared by exposing the culture to lysozyme. Smears from the resulting suspension of spheroplasts were prepared for the phase contrast microscopy.

The given approach was based on spectrophotometric measurements of the optical density of spheroplast owing to its change in the suspension at a wavelength of 540 nm. Also, the obtained spheroplast suspension was used for further preparation of smears for phase-contrast microscopy. Phase-contrast microscopy of *M. smegmatis* spheroplast smears isolated under the impact of lysozyme enzyme have shown that all the cells have transformed into spheroplasts as it is shown in Figure 2.

Measurements on Lambda 35 UV-spectrophotometer were performed for 30 min at 5 min interval. The given time exposition was applied based as the spheroplasts in the buffer solution survive not longer than for 30 min. FS-1 was applied in concentrations from 2 to 64 µg/mL, as at higher concentrations above 100 µg/mL the solution is getting dark due to the natural color of FS-1 that prevented any reliable measurement on the spectrophotometer. In the range of concentrations

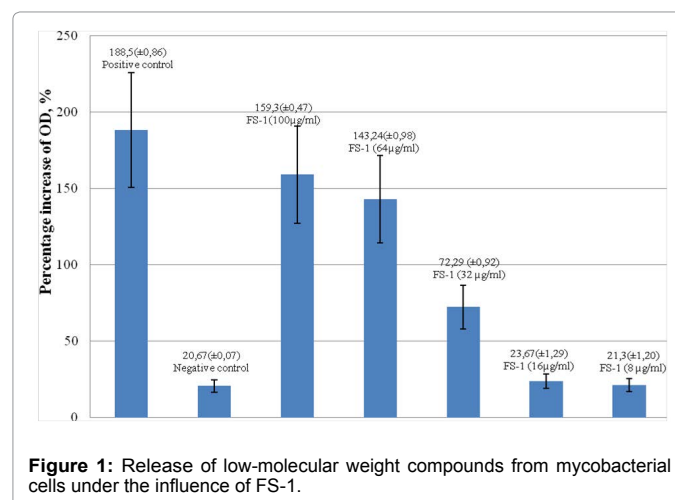


Figure 1: Release of low-molecular weight compounds from mycobacterial cells under the influence of FS-1.

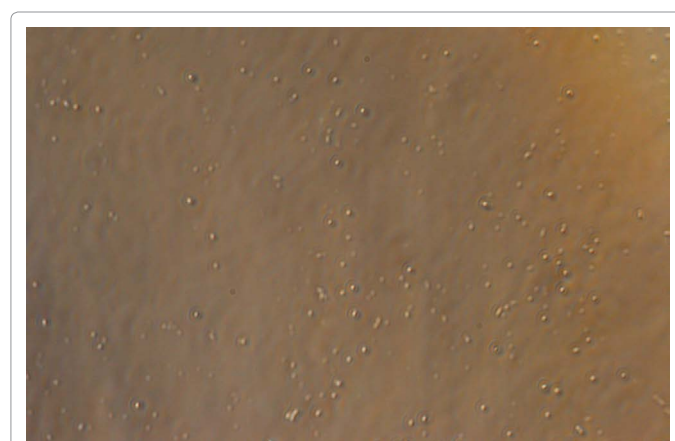


Figure 2: Spheroplasts obtained under the impact of lysozyme on *M. smegmatis* culture.

of 2-64 µg/mL the lytic activity of FS-1 on the spheroplasts was linear to the drug concentrations, i.e., the greatest spheroplast lysis was observed at the concentration of 64 µg/mL and the least – at 2 µg/mL, respectively, as it is shown on Figure 3.

Figure 3 shows that starting from the 5th min of the FS-1 exposure at the concentrations in the range of 4 to 64 µg/mL, the spheroplasts experienced a rapid lysis, which came to a complete lysis of the cells in 30 min. Whereas at the concentration of 2 µg/mL, the lysis by FS-1 has a weak manifestation that started only after 10 min of exposure.

Plating of the suspensions by inoculation also demonstrated the dose-dependent spheroplast lysis, as it is shown in Table 2.

Table 2 demonstrates that in 30 min of drug exposure at the concentration of 64µg/mL, the number of viable cells has reduced from 1.5×10^8 to 1.7×10^1 NMB/mL, i.e., by over 99.9% that confirms the lysis of the bacterial cell by FS-1.

Electron microscopy

In order to detect more profound changes of cell morphology of *M. tuberculosis* by the impact of FS-1, the electron microscopy was used. In this experiment, the strain *M. tuberculosis* 320 characterized by multiple drug resistance to rifampicin, isoniazid, streptomycin, ethambutol and pyrazinamide was used. A number of obtained photos of bacterial cells treated by FS-1 are shown in Figures 4-6.

Discussion

Molecular modeling

The structure of the FS-1 active center comprising a magnesium ion: The studied FS-1 complex contains molecular iodine, KI, LiCl(I), MgCl₂, polypeptides and α -dextrin.

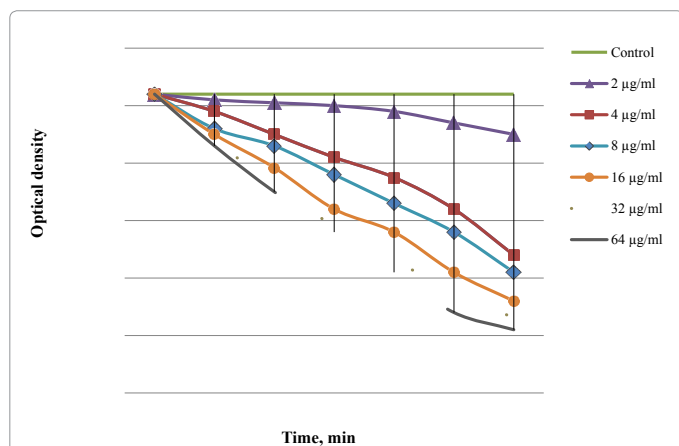


Figure 3: Lysis *M. smegmatis* ATCC 607 spheroplast exposed to FS-1.

Experimental conditions	Viable microorganism count, NMB/mL	
	before impact	30 min of impact
Control	1.5×10^8	1.5×10^8
2 µg/mL FS-1	1.5×10^8	3.8×10^7
4 µg/mL FS-1	1.5×10^8	2.3×10^3
8 µg/mL FS-1	1.5×10^8	1.8×10^3
16 µg/mL FS-1	1.5×10^8	5.1×10^2
32 µg/mL FS-1	1.5×10^8	3.1×10^1
64 µg/mL FS-1	1.5×10^8	1.7×10^1

Table 2: Control of the spheroplast lysis by plating.

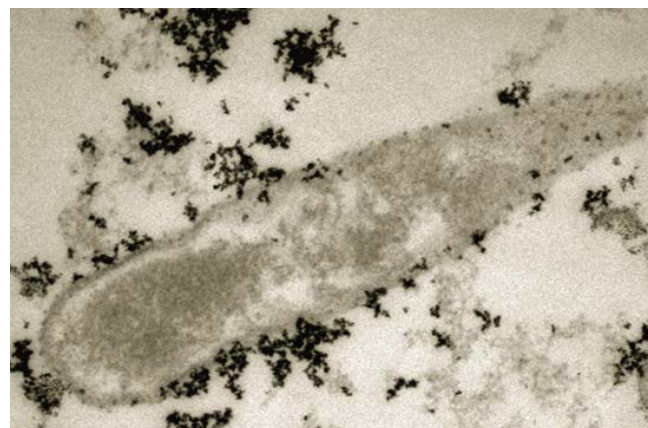


Figure 4: Accumulation of drug agent particles around a cell of *M. tuberculosis* on the cell wall followed by a destruction of the cell integrity and cytoplasm penetration.

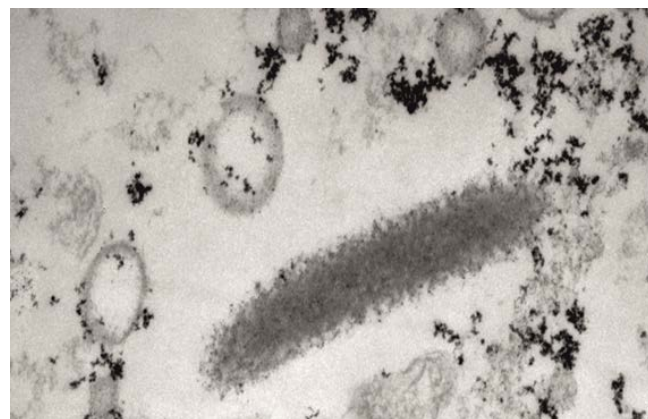


Figure 5: Bacterial cell filled internally with the drug FS-1. The cell wall and the cytoplasmic membrane are destroyed.

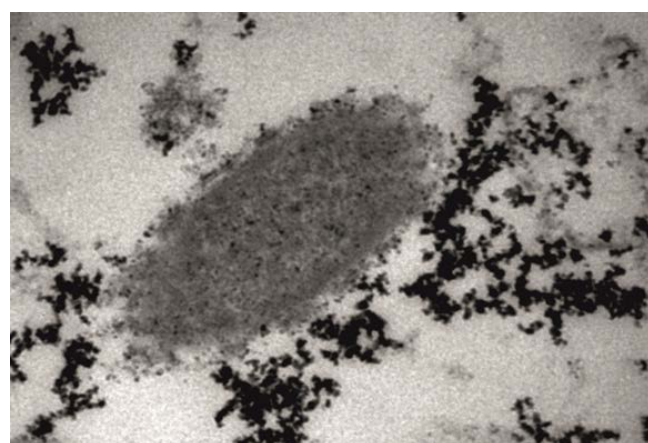


Figure 6: Destruction of the cell wall and cytoplasmic membrane leading to an outflow of the bacterial cell content.

In the entangled polymer complex, which is FS-1, physical methods of investigation cannot identify active centers of this drug. The structure of FS-1 active centers was studied on a model system of

its aqueous solution with potassium and lithium halogenide, molecular iodine, amino acid (glycine), ethanol ((a) system). Glycine was used in polypeptide modeling, ethanol – for α -dextrin. (a) System was studied using the methods of UV-IR-spectroscopy, UV-IR spectrums interpretation involved quantum-chemical method DFT/B3PW91 [2].

The analysis of UV spectra indicated that in aqueous solution of KI – I₂-amylose the number of rings of the dextrin helix may affect the iodine-triiodide equilibrium [13]. With the increase in the number of rings ($N \geq 15$), an existence of complexes of iodine and triiodide was detected in UV spectra. The α -dextrin, which is a part of FS-1, has 15 or more rings, therefore the complexes of iodine and triiodide could exist inside the helix.

The study revealed that glycine within the aqueous solution is located in zwitter-ion shape and it forms six molecule glycine clusters, being located under each other, thus, protonated amine group is positioned under a negatively-charged carboxyl group [2].

The cluster of glycine zwitter-ions, as well as α -dextrin helix, conditions the presence of I₂, I, I₃⁻ in the solution, that is why (a) system, which contains lithium halogenide may also represent the model of FS-1 drug.

Quantum-chemical calculations and spectroscopic studies indicate that there are three complexes formed in (a) system: In one of them – molecular iodine interacts with the oxygen atom of glycine carboxyl group and lithium halogenide, the second one – triiodine, forms the complex with protonated glycine amino group and as for the third one-lithium halogenide interacts with carboxyl group.

Above mentioned three complexes can also be formed inside of the α -dextrin helix and represent active centers of FS-1. LiCl(I)I₂-polypeptid complex and lithium halogenide are the strong acceptors and triiodine is the strong donor, that's why they can inhibit active enzymatic centers which are responsible for cell viability.

FS-1 structure also comprises magnesium halogenide. Magnesium ion may be located in α -dextrin helix and to be coordinated by OH group of α -dextrin. The most energetically preferable structure within the α -dextrin helix is the one that combines magnesium, triiodine ions and LiCl(I)I₂-polypeptde (complex I, Figure 7). The content

of magnesium ions in FS-1 is less than LiCl and I₂, for this reason α -dextrin helix would contain three mentioned complexes and Mg²⁺I₃⁻LiCl(I)I₂-polypeptide complexes (Figure 8).

Using DFT/CAM-B3LYP level with full geometry optimization, we calculated spatial and electronic structure of the complex I. In these calculations, polypeptide was replaced by amide and α -dextrin by ethanol.

In Figure 8, Blue balls-carbon atoms, red-oxygen atoms, blue-nitrogen atoms, violet-iodine atoms, green ball- magnesium ion and yellow-lithium ion.

Complex I is the binuclear complex represented by combination of magnesium and lithium ions with iodine ions (I⁵). Molecular iodine (I¹-I²) is positioned in α -dextrin helix and it is coordinated by lithium ion and peptide, located outside of α -dextrin helix. The interaction of magnesium ion with the triiodine results in the separation of triiodine into iodine ion and molecular iodine (I⁶-I⁴=3.54 Å, I³-I⁴=2.72 Å). Though I³-I⁴ does not display acceptor properties and can interact with neither with polypeptides or DNA nucleotides.

The UV spectrum of complex I was calculated by TD-DFT/CAM-B3LYP level.

As can be seen in Table 3, the theoretic wavelength within error

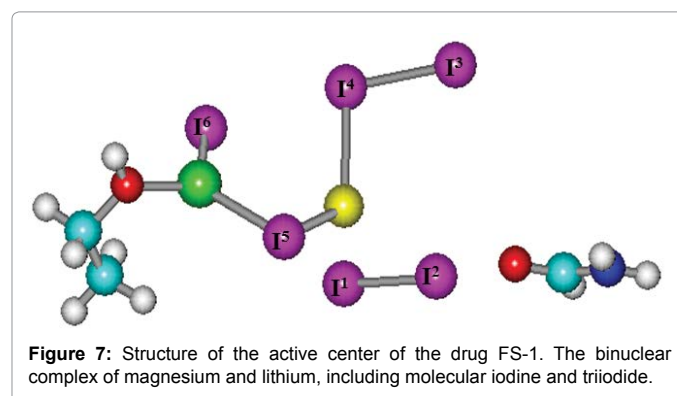


Figure 7: Structure of the active center of the drug FS-1. The binuclear complex of magnesium and lithium, including molecular iodine and triiodide.

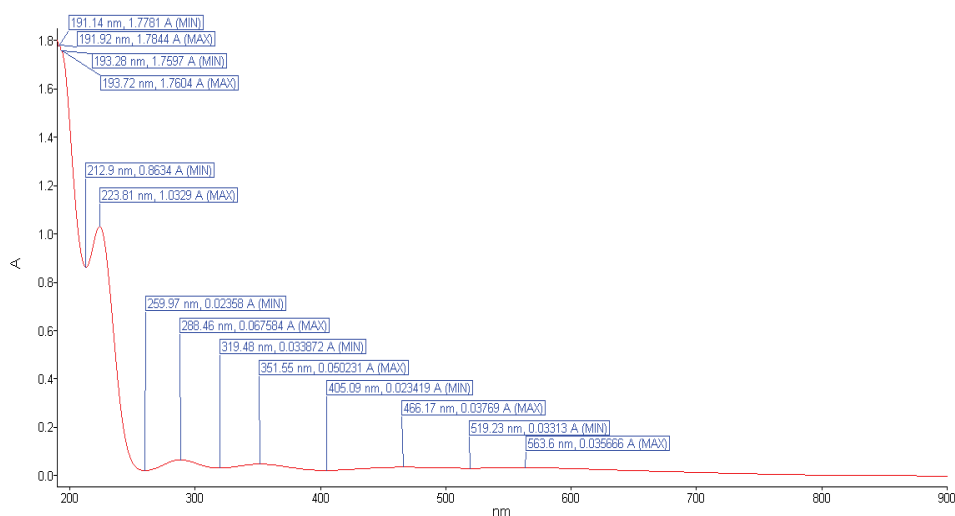


Figure 8: Experimental UV-spectrum of drug FS-1.

λ		f
221	${}^1A \rightarrow {}^1A (I^2, I^6, I^5) \rightarrow {}^*(I^1-I^2)$	0.2201
220	${}^1A \rightarrow {}^1A (I^1-I^2) \rightarrow {}^*(I^1-I^2)$	0.5412
275	${}^1A \rightarrow {}^1A (I^3-I^4, I^1-I^2) \rightarrow {}^*(I^1-I^2)$	0.1652
277	${}^1A \rightarrow {}^1A (I^1, I^5, I^6, I^3) \rightarrow {}^*(I^1-I^2)$ ${}^1A \rightarrow {}^1A (I^1-I^2) \rightarrow {}^*(I^1-I^2)$	0.2549

Table 3: Wavelengths of electronic transitions (λ , nm) oscillator strength (f).

method (~ 10 nm) is closely to the experimental FS-1 drug frequencies. This result indicates that complex I can be found in FS-1.

220 nm and 277 nm electronic transitions are the transitions from occupied MO to unoccupied MO I^1-I^2 . The distribution of electron density on the occupied by iodine atoms MO show that all the iodine atoms in complex I are bonded by delocalized electron density. The transition 275 nm is conditioned by the transfer of the delocalized electron density from occupied MO I^3-I^4, I^1-I^2 iodine atoms to the unoccupied I^1-I^2 orbital. 221 band is conditioned by the transfer delocalized electron density I^2, I^6, I^5 atoms to unoccupied I^1-I^2 orbital. The transfer of electron density from I^1, I^5, I^6 and I^3 orbital to unoccupied I^1-I^2 orbital also contributes 277 nm.

Within FS-1 structure, molecular iodine is protected from interaction with bioorganic ligands due to α -dextrin helix and polypeptide coordination. Only bioorganic ligands can compete with I_2 for complex formation as their donor activity towards iodine is higher of peptides. In our articles using quantum-chemical methods we have shown that only DNA nucleotides can compete with peptides for iodine complex formation [14]. UV-spectrum interpretation of aqueous solution, which contains FS-1 and nucleotide triplet, using TD-DFT/B3PW91 method indicates that nucleotides replace peptides from $LiCl(I)I_2$ polypeptdex complex and form the complex with molecular iodine and lithium halogenide [15].

We performed the calculation with full geometry optimization of complexes II a,b, in which DNA nucleotides and amides compete for iodine complex formation. As a result of geometry optimization, nucleotide replaces peptide and forms coordinate bond with molecular iodine. In our calculation peptide replaces by amide and α -dextrin by ethanol (Figure 9).

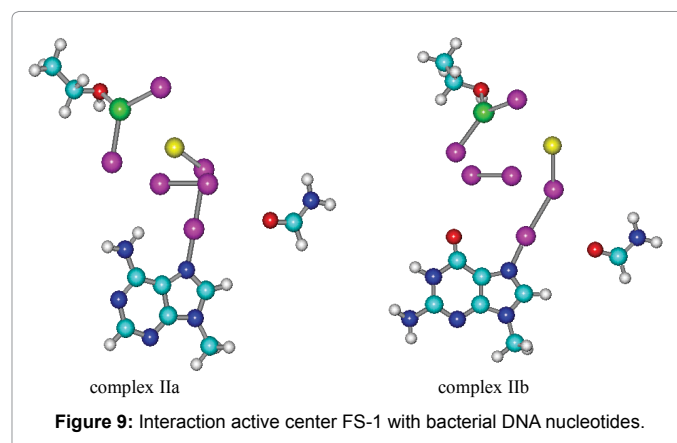
In Figure 9 blue balls-carbon atoms, red-oxygen atoms, blue-nitrogen atoms, violet-iodine atoms, green ball-magnesium ion and yellow-lithium ion.

Thus when FS-1 gets into bacterial intracellular compartment, its active centers protected from the interaction with the intracellular components by α -dextrin helix and coordination with polypeptide and they inhibit bacterial DNA nucleotides, which do not have protein coat.

Inhibition mechanism of DNA-dependent RNA-polymerase by the active FS-1 center containing magnesium ion: Using the method of molecular modeling we revealed the reason of experimentally proven antibacterial action of FS-1.

DNA-dependent RNA-polymerase (RNAP), using deoxyribonucleoside triphosphates (dATP, dGTP, dCTP, dTTP) as substrates, builds in nucleotides into the forming RNA chain according to the rules of complementarity, defining the unique position of the corresponding matrix nucleotide. The build-in of nucleotides is followed by the release of pyrophosphate, which lately undergoes enzymatic splitting, which brings almost irreversible character to polymerization reaction.

Unlike DNA-polymerases, which have separate active center for



DNA cleavage, all the reactions within RNAP take place in a single active center, which represents RNAP as the unique enzyme.

In the course of transcription, RNAP are able to implement multiple varied reactions: RNA synthesis, pyrophosphorolysis (nucleoside monophosphate transfer from the 3'-end of newly synthesized RNA to pyrophosphate that is followed by the formation of ATMP), also exo- and endonuclease digestion of RNA transcript (nucleoside monophosphate transfer (endonuclease) from the 3'-end of newly synthesized RNA, or several 3'-ended nucleotides to water molecule, which is followed by the formation of unoccupied LMF or short RNA fragment).

All these RNAP-based reactions take place according to the mechanism of bimolecular nucleophilic substitution (S_N2) and are implemented by active catalytic center.

X-ray data for RNAP represent the structure of active catalytic center. Its basic component comprises the site of three evolutionary invariant aspartic amino-acid residues, which are coordinated magnesium ion- $Mg^{2+}(COO)^3$ [16-19]. In equivalent to the small single subunit enzymes, it was postulated that the procedure of analysis involves two magnesium ions [20]. However the results of X-ray data represent contradictory information as for the second magnesium ion.

Sosunov et al. [20] in their article studied the structural and functional aspects of two Mg^{2+} ions within active catalytic center. Experimental results combined with molecular modeling lead to precise positioning of the second catalytic Mg^{2+} ion and point out the functional active center architecture, which explicates all the reactions of RNAP by means of a single unified mechanism.

They offered unified structural and functional model of an active center, which is in congruence with X-ray structure and determines all the activities of RNAP, exopyrophosphorylase and endopyrophosphorylase, exonuclease and endonuclease – the single mechanism based on the known geometry of S_N2 reaction. Pursuant to the model, phosphodiester bond breaking and synthesis is performed by the same active center. Both reactions involve the same symmetric Mg^{2+} ion pair, which alternates their roles in the coordination of donor and acceptor oxygen atoms during the interaction with phosphate nucleotide group (Figure 7 in [21]).

According to this data active catalytic center contains two magnesium ions. One of them are coordinated three aspartic amino-acid residues and has negatively-charge, other are coordinated one aspartic amino-acid residues and water molecular and has positive charge.

Using DFT/CAM-B3LYP level with full geometry optimization, we

calculated spacial and electronic structure of complex III (Figure 10), which models the interaction of active catalytic center of RNAP with phosphate group.

According to X-ray data, two magnesium ions are not bonded in a single binuclear complex within RNAP. They form binuclear complex only during interaction with phosphate group. Negative $Mg^{2+}(COO^-)_3$ ion can't interact with negatively-charged phosphate group, that's why the formation of binuclear complex III is implemented via two stages. During the first stage, positively-charged $Mg^{2+}COO^- \cdot H_2O$ ion coordinates negatively-charged phosphate group (complex IV, Figure 10), neutralizes its charge and forms the conditions for phosphate group interaction of the second magnesium ion- $Mg^{2+}(COO^-)_3$, the second stage involves $Mg^{2+}(COO^-)_3$ followed by the formation of complex III.

In Figure 10, blue balls-carbon atoms, red-oxygen atoms, blue-nitrogen atoms, violet-iodine atoms, green ball-magnesium ion, yellow-lithium ion, black ball-phosphorus atoms.

Within the process transcription of RNAP, DNA and forming RNA form ternary elongation complex (TEC). When FS-1 penetrate in bacterial cell cytoplasm its active center becomes the component of TEC. Magnesium ions of complexes II a,b, coordinated by molecular iodine and triiodine becomes the acceptor center, which can compete with phosphate RNA group for the complex formation with $Mg^{2+}(COO^-)_3$.

In the presence of FS-1 within bacterial cell cytoplasm, the TEC apart from IV complex also includes complexes IIa,b that can compete with complex IV for the complex formation with $Mg^{2+}(COO^-)_3$. We

calculated the bonding energies of $Mg^{2+}(COO^-)_3$ with complex IV ($\Delta E_1 = -55,5$ kcal/mol) and complexes IIa,b ($\Delta E_2 = -165,87$, $\Delta E_3 = -158,56$ kcal/mol). Calculations indicate the most stable complexes V a,b are formed in case if $Mg^{2+}(COO^-)_3$ is coordinated with complexes II a,b (Figure 11).

Thus, when active center FS-1 became the component of TEC the binuclear catalytic complex is not formed and the conditions ensuring transcription of the bacterial RNA are violated. Active center of FS-1 becomes center new nucleoprotein complex and bind both bacterial DNA and ion $Mg^{2+}(COO^-)_3$ of the active catalytic complex DNA dependent RNA polymerase. The conditions responsible for vital processes in the bacterial cell are violated. As a result, cell lysis is observed.

Conclusion

Findings of this research confirmed the expressed bactericidal activity against both the drug sensitive strain *M. tuberculosis* H₃₇Rv and the multi-drug resistant *M. tuberculosis* MS-115 at the concentrations from 8.2 $\mu\text{g/mL}$ to 2.7 $\mu\text{g/mL}$ during the entire investigation period (42 h).

The study of the release of low-molecular compounds from bacterial cells has shown that all the tested FS-1 concentrations increased the bacterial cell permeability to release low-molecular compounds into the culture fluid.

Spectrophotometry has shown that FS-1 penetrates through the cytoplasmic membrane and causes the lysis of cells (spheroplasts) partially devoid of the cell wall.

The quantum-chemical calculations carried out with the use of spectroscopic studies have shown that the effect on *M. tuberculosis* by the drug FS-1 is due to its ability to destroy the active catalytic complex of RNAP.

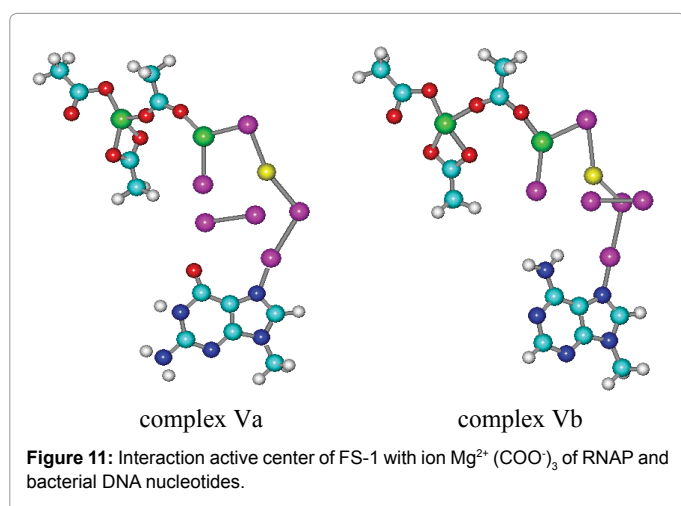
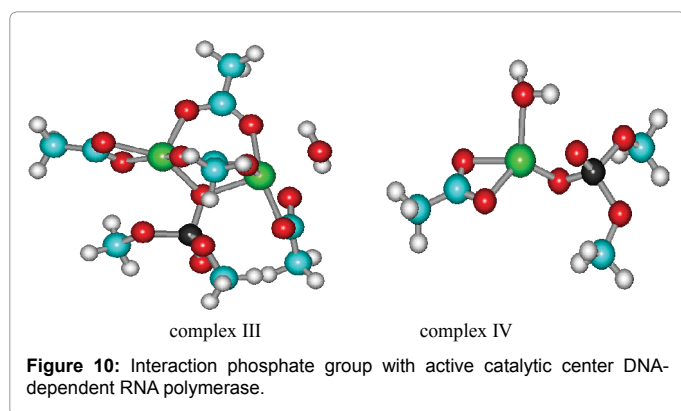
When the active center of FS-1 became the component of TEC, the binuclear catalytic complex of RNAP is not formed and the conditions ensuring transcription of the bacterial RNA are violated. Active center of FS-1 becomes the center of a new nucleoprotein complex and bind both bacterial DNA and ion $Mg^{2+}(COO^-)_3$ component of the active catalytic complex DNA dependent RNA polymerase. The conditions responsible for vital processes in the bacterial cell are violated. As a result, cell lysis is observed.

Acknowledgement

Calculations were made using a supercomputer at the National Laboratory for Information and Space Technologies (KazNRTU JSC).

References

1. Ilin A, Kulmanov M (2010) Description of invention antibacterial agent for treating infectious diseases of bacterial origin. Patent KZ No. 28746.
2. Yuldasheva G, Zhidomirov G, Leszczynski J, Ilin A (2016) Iodine containing drugs: Complexes of molecular iodine and tri-iodide with bioorganic ligands and lithium halogenides in aqueous solutions. In: Leszczynski J, Shukla M (2016) Practical Aspects of computational Chemistry IV chapter 10: 279-301.
3. Petrykina Z, Polin A, Belostotskaya, Komissarova N, Voleva B, et al. (1998) Antimicrobial and membrane-lytic activity of hindered phenols. *Antibiot Khimioter* 8: 11-15.
4. Yanai T, Tew D, Handy N (2004) A new hybrid exchange–correlation functional using the Coulomb-attenuating method (CAM-B3LYP). *Chem Phys Lett* 393: 51-57.
5. Gaussian 09, Revision D.01, M.J. Frisch et al. (Gaussian, Inc., Wallingford CT, 2009)



6. Tkachenko L, Verevkina O, Sviridova N, Lopatina I (2004) The use of the drug "Betadine" in bacterial vaginosis in the first trimester of pregnancy. *Gynecology* 2: 65-67.
7. Tyutyunnik V (2005) Pathogenesis, diagnosis and treatment of bacterial vaginosis. *Pharmateca* M 2: 20-24.
8. Boldyrev A, Kyaivyaryainen E, Ilyukha V (2006) Biomembranology. Teaching medium- petrozavodsk: Publ karelian scientific center of the Russian Academy of Sciences: 226.
9. Pepoyan A, Mirzoyan N, Saakyan M, Karagezan K (2001) Several antioxidative system peculiarities of *E. coli* G35 bacterial strains. *M Mole Boil*, pp: 65-69.
10. Kozlova N, Slobozhanina E, Antonovich A, Lukianenko L, Chernitsky E (2001) The impact of restored and oxidized glutathione on the physical-chemical status of erythrocyte membrane. *Biophysics* 3: 467-470.
11. Hofrichter M (2002) Review: Lignin conversion by manganese peroxidase (MnP). *Enz Micro Tech* 30: 454-466.
12. Bruce A, Johnson A, Lewis J, Raff M, Roberts K, et al. (2007) *Molecular biology of the cell*. 5th edition. New York: Garland Science.
13. Thoma J, French D (1960) The starch-iodine-iodide interaction. Part I. Spectrophotometric investigation. *J Am Chem Soc* 82: 4144-4147.
14. Yuldasheva G, Zhidomirov G, Ilin A (2012) Effect of organic ligands with conjugated π -bonds upon the structure of iodine- α -dextrin complexes. *Biotechnol Appl Biochem* 59: 29-34.
15. Yuldasheva G, Argirova R, Ilin A (2015) Inhibition of HIV-1 integrase active catalytic center by molecular iodine complexes with bioorganic ligands and lithium halogenides. *J AIDS Clin Res* 6: 2-6.
16. Zhang G, Campbell EA, Minakhin L, Richter C, Severinov K, et al. (1999) Crystal structure of *Thermus aquaticus* core RNA polymerase at 3.3 Å resolution. *Cell* 98: 811-824.
17. Korzheva N, Mustaev A, Kozlov M, Malhotra A, Nikiforov V, et al. (2000) A structural model of transcription elongation. *Science* 289: 619-625.
18. Cramer P, Bushnell D, Kornberg R (2001) Structural basis of transcription: RNA polymerase II at 2.8 Å resolution. *Science* 292: 1863-1876.
19. Vassilyev D, Sekine S, Laptenko O, Lee J, Vassilyeva M, et al. (2002) Crystal structure of a bacterial RNA polymerase holoenzyme at 2.6 Å resolution. *Nature* 417: 712-719.
20. Steitz T (1998) A mechanism for all polymerases. *Nature* 391: 231-232.
21. Sosunov V, Sosunova E, Mustaev A, Bass I, Nikiforov V, et al. (2003) Unified two-metal mechanism of RNA synthesis and degradation by RNA polymerase. *EMBO J* 22: 2234-2244.